2021 43rd Annual International Conference of the
IEEE Engineering in Medicine & Biology Society (EMBC)
Oct 31 - Nov 4, 2021. Virtual Conference

Development of DTI Based Probabilistic Tractography Methods to Characterize Arm Muscle Architecture in Individuals Post Hemiparetic Stroke

Divya Joshi, Julius P.A. Dewald, *Member, IEEE*, and Carson Ingo

***Abstract*— A hemiparetic stroke may lead to changes in muscle structure that further exacerbate motor impairments of the paretic limb. Cadaveric measurements have previously been used to study structural parameters in skeletal muscles but has several limitations, including *ex vivo* fixation. Here, we present novel application of diffusion tensor imaging (DTI) based probabilistic tractography methods, in comparison to the traditional deterministic approach, with respect to cadaveric dissection to quantify *in vivo* muscle fascicles in the biceps brachii. Preliminary results show that probabilistic tractography yields longer fascicle lengths that are more consistent with cadaveric measurements, albeit with higher variability, while deterministic tractography identifies shorter fascicle lengths, but with less variability. Results suggest that DTI tractography techniques can capture fascicles consistent with previously published cadaveric measurements and can identify interlimb differences in fascicle lengths in an individual with stroke.**

***Clinical Relevance*— The methods proposed here describe a non-invasive way to quantify heterogeneous musculoskeletal parameters such as across upper arm muscles in individuals with hemiparetic stroke. This will expand the current knowledge of macro- and micro-structural muscle changes that occur after stroke and may lead to more effective rehabilitation strategies to prevent such changes in individuals with stroke.**

I. Introduction

Skeletal muscles are influenced by and adapt based on neural input patterns and activity levels. A hemiparetic stroke disrupts typical drive of the muscle which results in reduced use of the paretic limb [1]. Motor deficits following stroke have been shown to be closely related to changes in muscle structure, such as reduced fascicle length [3-4]. This may lead to changes in muscle architecture that can further exacerbate the functional use of the paretic limb.

Traditionally, structural parameters of skeletal muscles, such as fascicle lengths and pennation angles, have been studied using measurements made on cadaver specimens. Cadaveric methods allow identification of more complicated and varying architectural parameters, but pose limitations such as *ex vivo* fixation, limited availability, and lengthy measurement time [4]. More recently, ultrasound has been used to non-invasively capture *in vivo* muscle but has a field of view limited to superficial located regions of muscles [5]. Ultrasonic methods therefore tend to yield a small and unvaried sample of measurements.

To overcome limitations posed by cadaveric and US measurements, magnetic resonance (MR) based diffusion tensor imaging (DTI) tractography has emerged as an *in vivo* approach that is able to non-invasively estimate musculoskeletal architecture across superficial and deep muscles. DTI measures the random thermal displacement of water molecules within biological tissues, which preferentially diffuse along the primary orientation of anisotropic tissue. Thus, DTI tractography can probe architecture of muscle fibers or fascicles, which allows for estimation of geometric features within skeletal muscles [6].

There have been limited studies of DTI deterministic tractography to characterize skeletal muscle; almost all have focused on leg musculature in healthy individuals [5, 7–9] or in individuals with neuromuscular disorders [10–13]. With the exception of one study [14], there has been no work that implements DTI tractography in arm muscles. Furthermore, establishing the feasibility of such a technique in a pathophysiological context, such as following a stroke, is particularly important as the muscle tissue may be affected, influencing imaging metrics, such as signal-to-noise ratio, accuracy of fiber tracking, which need to be accounted for during data collection, processing, and analysis.

DTI tractography is implemented with either deterministic algorithms to compute a binary decision for tract reconstruction based on primary diffusion direction in contiguous voxels, or probabilistic algorithms, which compute a likelihood for tract reconstruction based on primary diffusion direction in contiguous voxels [15]. In the brain, it has been shown that probabilistic tractography can more reliably distinguish crossing fibers [16]. However, for skeletal muscle, there has been no investigation into the differences between the two DTI tractography methods [4]. An examination of the two methods is necessary so that future work using skeletal muscle DTI can produce robust and anatomically reasonable results.

This paper focuses on novel *in vivo* DTI tractography methods developed to quantify muscle fascicle lengths and organization, which show consistency with results reported

*Research supported by NIH Grants R01 HD084009 and T32 EB025766.

D. Joshi is with the departments of Biomedical Engineering and Physical Therapy and Human Movement Sciences at Northwestern University, Chicago, IL 60611, USA (phone: 312-908-8160; fax: 312-908-0741; e-mail: divyajoshi@u.northwestern.edu).

C. Ingo is with the departments of Physical Therapy and Human Movement Sciences and Neurology at Northwestern University, Chicago, IL 60611, USA (e-mail: carson.ingo@northwestern.edu).

J.P.A. Dewald is with the departments of Physical Therapy and Human Movement Sciences, Biomedical Engineering and Physical Medicine Rehabilitation, and at Northwestern University, Chicago, IL 60611, USA (e-mail: j-dewald@northwestern.edu).

using traditional *ex vivo* cadaveric methods. The methods presented here, based on muscles from one control individual and two individuals with stroke, can be expanded upon to investigate the impact of a hemiparetic stroke on the macro- and micro-structure of skeletal muscle tissue.

II. Methods

The primary objective of the following experimental protocol and data analysis was to establish a pipeline that feasibly images and extrapolates muscle fascicles in the upper arm. We integrated three steps, which together reconstruct muscle fascicles and ensure high quality and anatomically sound estimates of structural parameters in skeletal muscles of the arm. The Northwestern Institutional Review Board approved of all experimental procedures described here.

A. Scanning Parameters and Setup

Diffusion Tensor Imaging

MR images of participants' uppers arms were acquired on a 1.5T Siemens Aera scanner (Siemens Medical Systems Inc, USA) with a 2x18 channel body matrix coil placed around the upper arm. Participants will lay on their side with the arm being imaged positioned with the shoulder at neutral, the elbow at 165° extension (with 180° being full extension), and the forearm in mid pronation-supination (Fig. 1A). This position allows for the upper arm to be as close to the center of the scanner as possible, capturing the muscles of interest in the field of view and minimizing image artifacts from B_0 inhomogeneities.

Structural T1-weighted scans were acquired using a high-resolution 3D VIBE sequence with the following parameters: TR=16 ms, TE=7.16 ms, FOV=256x304 mm^2, slice thickness=3 mm, and voxel resolution=0.78x0.78x3 mm^3. Diffusion weighted images were acquired using a spin-echo echo-planar imaging sequence with the following parameters: TR=8500 ms, TE=48 ms, FOV=250x250 mm^2, slice thickness=5 mm, and voxel resolution=1.25x1.25x5 mm^3. Imaging included Spectral Attenuated Inversion Recovery (SPAIR) fat suppression. The diffusion weighted scan included 12 diffusion-weighted directions with a b-value of 400 s/mm^2 with 3 averages each, as well as 10 scans with no diffusion weighting (b=0 s/mm^2). The TE and b-values chosen are optimized for diffusion MRI in skeletal muscle [17].

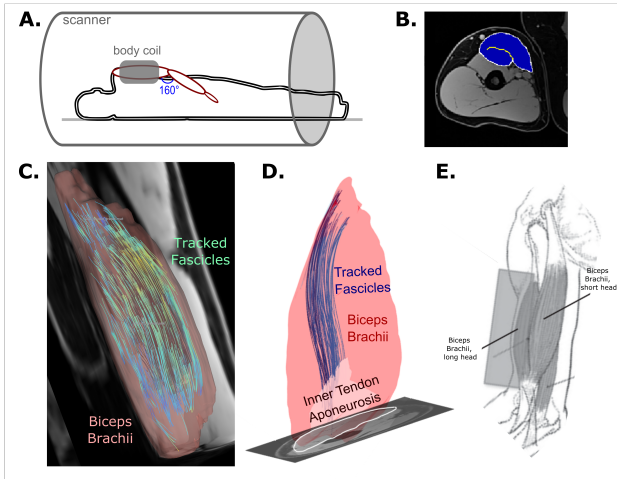

Figure 1. (A) Participant positioning in 1.5T MR scanner. **(B)** Segmentations of biceps brachii muscle outline (white), inner tendon aponeurosis (yellow), and whole muscle seed region (blue). **(C)** Examples of deterministically generated tracts seeded from the whole muscle. **(D)** Examples of probabilistically generated tracts seeded from the whole muscle. **(E)** Anatomical rendering of the biceps brachii muscle [2].

B. Data Processing and Tractography

Image Pre-Processing

Pre-processing of MR data was done using the FSL software library [18]. First, extraction was performed to isolate only the arm region in all volumes. Next, data was denoised using previously published algorithms [19]. Linear registration was performed using FLIRT. All images were linearly registered to images without a diffusion weighting to minimize motion artifacts. The 10 volumes with no diffusion weighting were then averaged together to create a baseline image. Eddy current distortions were corrected for with affine registration, and diffusion gradient directions were corrected for.

Anatomical T1 images guided identification and segmentation of the biceps brachii muscle and its inner tendon aponeurosis in both arms (Fig. 1B). T1 segmentations were registered to the diffusion scan space and later used during tractography as regions of interest for fiber tracking initiation and termination.

Deterministic Tractography

Deterministic tractography was performed using the DSI Studio software [20]. A deterministic fiber tracking algorithm was performed with the following parameters: angular threshold=10°, step size=0.5 mm, and minimum length=20 mm. Fiber tracking was initiated bidirectionally at points within the selected seedmask (segmentation of the whole biceps muscle) and terminated at the outer boundaries of the biceps and/or the inner tendon aponeurosis (Fig. 1C).

Probabilistic Tractography

Probabilistic tractography and fiber tracking were performed using the BEDPOSTX and PROBTRACKX algorithms, respectively, using the FSL software library [18]. BEDPOSTX, which uses Bayesian estimation methods to grow potential tracts, was performed with the following parameters: maximum fibers per voxel=2, burnin period=1000, and step size=0.5 mm. PROBTRACKX was initiated bidirectionally at points within the selected seedmask (segmentation of the whole biceps muscle) and terminated at the outer boundaries of the biceps and/or the inner tendon aponeurosis (Fig. 1D).

C. Reconstruction of Muscle Fascicles

Custom-written MATLAB code was used to generate anatomically reasonable (see Fig. 1E) muscle fascicle representations from raw tracts output by DTI tractography and to estimate lengths of the muscle fascicle representations. These steps are described below.

Calculation of Fascicle Lengths

Polynomial interpolation and least squares fitting were used to fit the tracts to third order polynomial curves, which represented the muscle fascicles. These curves were used to calculate length of the fascicles.

Anatomical Acceptance Criteria for Valid Tracts

For probabilistically generated tracts, anatomical points were extracted by identifying the coordinates of the voxel with the highest probability of diffusion in each slice and were transformed to anatomical space. In each tract, the longest consecutive tracked set of coordinates was used. For deterministically methods, the set of points making up each tract was transformed to anatomical space as defined by the T1 image. For both methods, tracts with lengths less than the defined minimum length (deterministic: 20 mm, probabilistic: 30% of the muscle belly length) were discarded. The remaining tracts represented the reconstructed muscle fascicles that were used in further analysis.

Normalization of Fascicle Lengths for Comparison to Cadaveric Data

The muscle belly length of the biceps brachii was calculated as the Euclidean distance between the origin and insertion of the biceps brachii muscle. All calculated fascicle lengths were divided by the biceps belly length to normalize the estimates to the size of the corresponding muscle.

Murray et al. measured 10 fascicle lengths in each of six dissected biceps brachii muscles, which were then normalized to the optimal sarcomere length in the human muscle to generate a range of optimal fascicle lengths of the biceps brachii [21]. For comparison to DTI tractography, a normal distribution of six cadaveric estimated fascicle lengths was simulated based on the normalized fascicle length mean and standard deviation reported by Murray et al.

III. Preliminary Results

A preliminary study of two individuals with hemiparetic stroke and one healthy individual was carried out to investigate: (1) whether DTI tractography produced results consistent with previously published cadaveric measurements conducted in the same individuals and (2) if the tractography algorithm used had an impact on the fascicle length estimates and variability.

Preliminary findings from both probabilistic tractography and deterministic tractography initiated from a whole muscle seed region were compared to published fascicle lengths measured from cadavers (Fig. 2). The distribution of cadaveric fascicle lengths distribution was based upon 10 fascicles measured per muscles across six biceps muscles dissected from different individuals, while DTI distributions looked at about 100 fascicles per muscle within the same individual. A one-way analysis of variance was used to compare normalized fascicle lengths between the three methods. There was a significant difference between length estimates generated by both deterministic and probabilistic tractography and cadaveric methods (p=0.0003 and p=0.022, respectively). However, there was no significant difference between the tractography methods (p=0.124) (Fig. 2).

As shown in both Fig. 2 and Table 1, probabilistic methods, but not deterministic methods, generated a wide range in estimated fascicle lengths, similar to that seen in the cadaver data. Table 1 shows an examination of the coefficient of variance in the three methods in each muscle scan. The coefficients of variance for the probabilistic tractography and the cadaveric results are on the order of 0.2 to 0.3, while the coefficient is much smaller at 0.075 (Table 1).

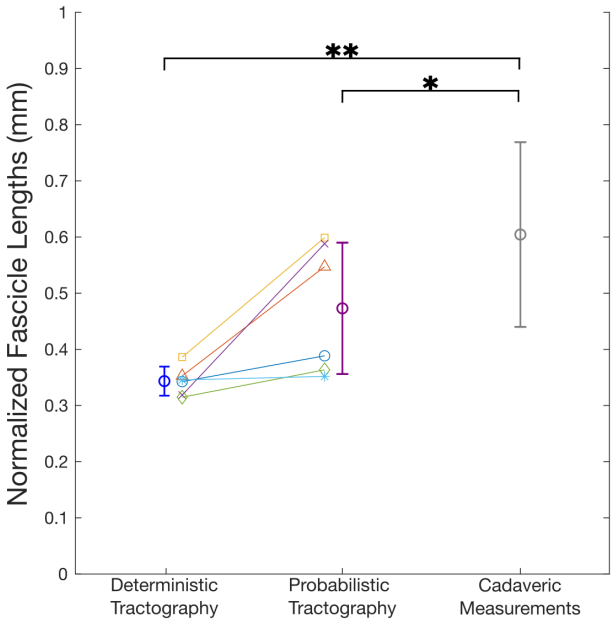

Figure 2. Normalized fascicle lengths of the biceps brachii, normalized to muscle belly length (n=6). Length estimates are obtained from deterministic DTI tractography (mean ± SD in blue) and probabilistic DTI tractography (mean ± SD in purple). A simulated distribution of fascicle lengths measured from 6 arms based on previously published results by Murray et al [21] is shown (mean ± SD in grey). A * indicates $p < 0.05$ and a ** indicates $p < 0.01$.

IV. Discussion

This paper introduces the novel DTI application of using probabilistic tractography to quantify *in vivo* muscle fascicles in upper arm muscles. Preliminary results also show that probabilistic and deterministic tractography algorithms consistently yield different fascicle length estimates with contrasting ranges (Fig. 2). The deterministic approach produces shorter fascicle lengths and demonstrates less variance, while the probabilistic approach estimates longer fascicle lengths with higher variance. As shown in Table 1, the higher variance in the probabilistic method are more similar to cadaveric measurements, in comparison to the deterministic results [21].

While there is no true gold standard for capturing *in vivo* muscle structural parameters, cadaver dissections have been historically used to obtain *ex vivo* measurements. The agreement in length estimates and variability between probabilistic methods and results from cadaver dissection indicates that probabilistic tractography is potentially better suited to reliably identify heterogeneous skeletal muscle structure in the upper arms. Furthermore, previous cadaveric work has shown evidence that parallel fibered muscles, such

Table 1. Coefficients of variances (CoV) of fascicle length estimates produced by three methods: deterministic tractography, probabilistic tractography, and previously published cadaveric measurements [21].

CoV Across Length Estimation Methods

Deterministic Tractography	***Probabilistic Tractography***	***Cadaveric Measurements*** [21]
0.075	0.247	0.272

as the biceps brachii, have a complex arrangement of fibers, and that some fibers are arranged in series to transmit force between one another [22]. The greater range in fascicle lengths estimated by probabilistic methods indicates that the technique is capturing fascicles of varying geometry, illustrating the complex structural organization. Therefore, the proposed methods suggest a promising ability to capture intricate anatomical details that have previously only been studied with cadaveric dissections.

Additionally, it has been shown that there are changes to skeletal muscle organization following a stroke, due to the highly plastic nature of skeletal muscle [23]. Therefore, stroke-induced pathophysiology may affect and alter complex fascicle arrangements, as well as other musculoskeletal parameters. The use of probabilistic tractography in individuals with stroke would not only allow demonstration of the shortening of fascicles post-stroke, which has been previously shown using ultrasound [2], but additionally illustrate the potential reorganization of muscle fascicles that may take place after a hemiparetic stroke.

V. Conclusion

This paper offers a novel, non-invasive experimental design and data analysis process to quantify *in vivo* musculoskeletal architecture in upper arm musculature. It presents preliminary results showing that probabilistic tractography may be more consistent with traditional *ex vivo* cadaveric measurements than deterministic methods and is a promising *in vivo* approach to identify interlimb differences in musculoskeletal architecture in individuals with stroke. It should be noted that these results are limited to only three participants (six muscles) and a larger sample size is necessary. Additionally, further investigation is required to optimize the tractography parameters to ensure validity of reconstructed muscle fascicles that are specific to the muscle group of interest. Future work will apply these non-invasive methods to study how hemiparetic stroke affects fascicle lengths, as well as pennation angles and curvature. Additionally, the proposed methods will be used to examine diffusivity metrics within the muscle, giving insight into microstructural changes of the skeletal muscle tissue induced by post stroke limb disuse. Application of the techniques described here will lead to a more comprehensive understanding of the musculoskeletal structural adaptations that follow a hemiparetic stroke.

Acknowledgment

We would like to thank Marie Wasielewski for her assistance in MR imaging.

References

[1] M. Owen, C. Ingo, and J. P. A. Dewald, "Upper Extremity Motor Impairments and Microstructural Changes in Bulbospinal Pathways in Chronic Hemiparetic Stroke," *Front. Neurol.*, vol. 8, p. 257, Jun. 2017.

[2] C. M. Nelson, W. M. Murray, and J. P. A Dewald, "Motor Impairment–Related Alterations in Biceps and Triceps Brachii Fascicle Lengths in Chronic Hemiparetic Stroke," 2018.

[3] A. N. Adkins, J. P. A. Dewald, L. Garmirian, C. M. Nelson, and W. M. Murray, "Serial sarcomere number is substantially decreased within the paretic biceps brachii in chronic hemiparetic stroke," *bioRxiv*, p. 2020.03.12.989525, Mar. 2020.

[4] B. M. Damon *et al.*, "Skeletal muscle diffusion tensor-MRI fiber tracking: rationale, data acquisition and analysis methods, applications and future directions.," *NMR Biomed.*, vol. 30, no. 3, Mar. 2017.

[5] B. Bolsterlee, T. Finni, A. D'Souza, J. Eguchi, E. C. Clarke, and R. D. Herbert, "Three-dimensional architecture of the whole human soleus muscle in vivo," *PeerJ*, vol. 6:e4610, Apr. 2018.

[6] D. Le Bihan *et al.*, "Diffusion tensor imaging: Concepts and applications," *J. Magn. Reson. Imaging*, vol. 13, no. 4, pp. 534–546, Apr. 2001.

[7] B. Bolsterlee, H. E. J. Veeger, F. C. T. Van Der Helm, S. C. Gandevia, and R. D. Herbert, "Comparison of measurements of medial gastrocnemius architectural parameters from ultrasound and diffusion tensor images," *J. Biomech.*, vol. 48, no. 6, pp. 1133–1140, Apr. 2015.

[8] B. Bolsterlee, A. D'Souza, S. C. Gandevia, and R. D. Herbert, "How does passive lengthening change the architecture of the human medial gastrocnemius muscle?," *J. Appl. Physiol.*, vol. 122, no. 4, pp. 727–738, Apr. 2017.

[9] B. Bolsterlee, A. D'souza, and R. D. Herbert, "Reliability and robustness of muscle architecture measurements obtained using diffusion tensor imaging with anatomically constrained tractography," *J. Biomech.*, vol. 86, pp. 71–78, 2019.

[10] A. D'souza, B. Bolsterlee, A. Lancaster, and R. D. Herbert, "Muscle architecture in children with cerebral palsy and ankle contractures: an investigation using diffusion tensor imaging," *Clin. Biomech.*, vol. 68, pp. 205–211, 2019.

[11] A. D'Souza, B. Bolsterlee, and R. D. Herbert, "Architecture of the medial gastrocnemius muscle in people who have had a stroke: A diffusion tensor imaging investigation," *Clin. Biomech.*, vol. 74, pp. 27–33, Apr. 2020.

[12] A. S. Sahrmann, N. S. Stott, T. F. Besier, J. W. Fernandez, and G. G. Handsfield, "Soleus muscle weakness in cerebral palsy: Muscle architecture revealed with Diffusion Tensor Imaging," *PLoS One*, vol. 14, no. 2, p. e0205944, Feb. 2019.

[13] M. T. Hooijmans *et al.*, "Evaluation of skeletal muscle DTI in patients with duchenne muscular dystrophy," *NMR Biomed.*, vol. 28, no. 11, pp. 1589–1597, Nov. 2015.

[14] M. Froeling *et al.*, "Diffusion-tensor MRI reveals the complex muscle architecture of the human forearm," *J. Magn. Reson. Imaging*, vol. 36, no. 1, pp. 237–248, 2012.

[15] T. Sarwar, K. Ramamohanarao, and A. Zalesky, "Mapping connectomes with diffusion MRI: deterministic or probabilistic tractography?," *Magn. Reson. Med.*, vol. 81, no. 2, pp. 1368–1384, Feb. 2019.

[16] J. M. Soares, P. Marques, V. Alves, and N. Sousa, "A hitchhiker's guide to diffusion tensor imaging," *Front. Neurosci.*, vol. 7, no. 7 MAR, 2013.

[17] N. Saupe, L. M. White, J. Stainsby, G. Tomlinson, and M. S. Sussman, "Diffusion Tensor Imaging and Fiber Tractography of Skeletal Muscle: Optimization of b Value for Imaging at 1.5 T," *Am. J. Roentgenol.*, vol. 192, no. 6, pp. W282–W290, Jun. 2009.

[18] S. M. Smith *et al.*, "Advances in functional and structural MR image analysis and implementation as FSL," *Neuroimage*, vol. 23, no. SUPPL. 1, pp. 208–219, 2004.

[19] S. Aja-Fernández, C. Alberola-López, and C. F. Westin, "Noise and signal estimation in magnitude MRI and Rician distributed images: A LMMSE approach," *IEEE Trans. Image Process.*, vol. 17, no. 8, pp. 1383–1398, Aug. 2008.

[20] F.-C. Yeh, T. D. Verstynen, Y. Wang, J. C. Fernández-Miranda, and W.-Y. I. Tseng, "Deterministic Diffusion Fiber Tracking Improved by Quantitative Anisotropy," *PLoS One*, vol. 8, no. 11, p. e80713, Nov. 2013.

[21] W. M. Murray, T. S. Buchanan, and S. L. Delp, "The isometric functional capacity of muscles that cross the elbow," *J. Biomech.*, vol. 33, no. 8, pp. 943–952, Aug. 2000.

[22] G. E. Loeb, C. A. Pratt, C. M. Chanaud, and F. J. R. Richmond, "Distribution and innervation of short, interdigitated muscle fibers in parallel-fibered muscles of the cat hindlimb," *J. Morphol.*, vol. 191, no. 1, pp. 1–15, Jan. 1987.

[23] L. L. Ploutz-Snyder, B. C. Clark, L. Logan, and M. Turk, "Evaluation of Spastic Muscle in Stroke Survivors Using Magnetic Resonance Imaging and Resistance to Passive Motion," *Arch. Phys. Med. Rehabil.*, vol. 87, no. 12, pp. 1636–1642, Dec. 2006.